MIMO Antenna and Beamforming Algorithm Based on Characteristic Mode of Bilateral Symmetric Structure

Dong-Woo Kim, and Sangwook Nam

INMC, Seoul National University, Korea

***Abstract*—There are various bilaterally symmetric structures in the world. Characteristic mode analysis (CMA) enables to use a conductor with the symmetric structure itself as an antenna. Based on CMA, it is possible to implement a multiport MIMO antenna on the conductor using a mode-decoupling network (MDN). As the number of antennas increases, however, the complexity of the MDN becomes large, making design difficult. In this paper, we propose a simpler systematic design method for a multiport MIMO antenna on an electrically small and bilaterally symmetric conductor. More specifically, the implementation of the MDN depends on the design of the coupling elements that excite characteristic modes, so a design method for its position and shape is proposed. Owing to the well-designed coupling elements, a simple systematic design of the multiport MIMO antenna is suggested. In addition to the MIMO application, the beamforming algorithm is investigated using the proposed multiport antenna.**

***Index Terms*—Bilateral symmetry, characteristic current point correlation, characteristic mode analysis (CMA), MIMO antenna, mode-decoupling network (MDN), platform-mounted antenna.**

I. Introduction

MUCH effort is being devoted to increasing the data rate of today's communication systems. One way to increase capacity is by using multiple-in-multiple-out (MIMO) communication [1], which can enhance capacity without broadening bandwidth. However, obtaining higher increases in channel capacity for an increase in the number of inputs or outputs requires some conditions to be met. In antenna design, uncorrelation and high isolation should be ensured between the antennas [1]. However, these features become more difficult to ensure as the distance between antennas diminishes.

Characteristic mode analysis (CMA) is a suitable theory for an antenna design [2], [3]. It provides physical insights into the characteristics of an antenna, and therefore, can be applied to platform-mounted antenna designs [4]-[6]. This type of antenna can be designed intuitively by placing a coupling element for exciting a particular mode derived from CMA of the antenna platform. In addition, CMA also provides a set of basis currents that guarantee the orthogonality of the far-field patterns; therefore, it has been proposed for usage with various antennas for MIMO applications [7]-[14]. From the orthogonal property, matching each characteristic mode (CM) with an MIMO element antenna gives a low pattern correlation, which can be used for pattern diversity based MIMO antenna. Specifically, a 2-port MIMO antenna can be implemented through nothing more than proper design of coupling elements [7]-[10]. However, in the case of a multiport MIMO antenna design, individual excitation of each CM becomes difficult as more CMs are involved, because they are intertwined each other. For this reason, an additional mode-decoupling network (MDN) is required.

In fact, researches showed that the design of multiport MIMO antennas can be realized by constructing an MDN that is derived from eigenvalue decomposition of the Z-matrix or S-matrix of the antenna ports [15]-[17]. Like CMA, the antenna patterns created through the designed MDN also provide orthogonality. However, as the number of antennas grows, the complexity of the MDN increases considerably [17], and sometimes a certain amount of loss is required in the network [15]. In [16] and [17], it was suggested that the MDN can be easily implemented through symmetric design of the antennas and ports. On the other hand, studies combining the MDN and CMA were also conducted in [11] and [18]. In [18], it was shown that patterns of the MIMO antenna generated through the MDN derived from the Z-matrix coincide with the combination of the modal patterns, rather than each individual modal pattern. In [11], it was suggested that a simple MDN configuration is possible when the ports to excite CMs are designed symmetrically on a symmetric conductor. However, a multiport MIMO antenna design based on the method used in [11] requires a biaxially symmetric structure as shown in Fig. 1-(a).

In this paper, a simple method of designing a multiport MIMO antenna using CMA and MDN on an electrically small conductor with bilateral symmetry as shown in Fig. 1-(b) is proposed, which is conceptually introduced in [19]. Since the design of the MDN and excitation of the CMs are determined by the coupling elements, a design method for these positions and shapes is suggested. In the case of a bilaterally symmetric conductor, CMs are classified into two groups, an even CM and an odd CM. Antennas using the different CM groups (even and odd CMs) can be separated by designing coupling elements using structural symmetry. For a multiport extension, the separation between antennas using the same CM group (even or

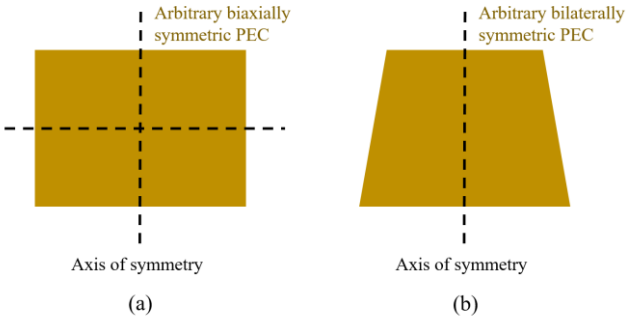

Fig. 1. Examples of (a) biaxially symmetric conductor, and (b) bilaterally symmetric conductor.

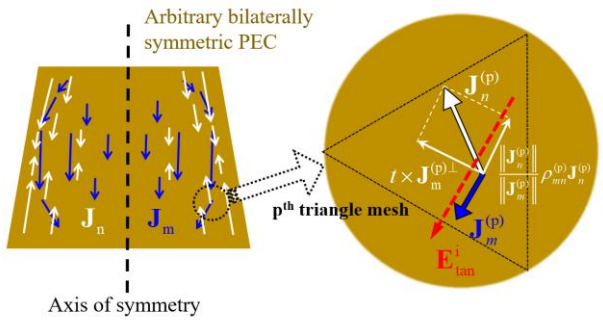

Fig. 2. Illustrative explanation of the vector notations of characteristic currents and assumed incident tangential E-field.

odd CMs) is required. However, since the mode currents in the same CM group are usually correlated, separating these antennas with only the coupling elements is difficult, so an additional MDN is required. However, owing to the separation of antennas using the different CM groups, the MDN can be constructed more easily than the conventional MDN design method used in [15]. As a result, a systematic design of a 3-port MIMO antenna can be possible only with one conventional unequal 180° hybrid coupler for the MDN. For a 4-port MIMO antenna with two even CMs and two odd CMs, the design can be possible using two unequal 180° hybrid couplers.

The paper is organized as follows. In section II, the theory of characteristic mode analysis is reviewed, the characteristic current point correlation is defined, the physical meaning of this correlation is found, and the coupling element is briefly reviewed. In section III, the properties mentioned in section II are applied to the positioning and shaping of the coupling elements. Also, a systematic design approach using MDN is developed for a multiport electrically small and bilaterally symmetric MIMO antennas. In section IV, the capabilities of beamforming are suggested using the proposed multiport antenna. In section V, conclusions about the finding are drawn.

II. Theory

A. Characteristic mode analysis (CMA)

The theory of the characteristic mode (CM) of conducting bodies was first introduced by Garbacz in 1968 [2], and later refined by Harrington and Mautz in 1971 [3]. It provides a basis set of current on the body, which has orthogonal properties of radiation. These basis currents are called characteristic currents, and they are determined by the following a generalized eigenproblem:

$$\mathrm{X}\mathbf{J}_\mathrm{n} = \lambda_\mathrm{n}\mathrm{R}\mathbf{J}_\mathrm{n} \tag{1}$$

where λ_n is eigenvalue, $\mathbf{J}_\mathrm{n}$ is characteristic current, and R and X are the real and imaginary parts of the MoM Z-matrix of the conductor. Since R and X are the real and symmetric matrices, all eigenvalues λ_n and characteristic currents $\mathbf{J}_\mathrm{n}$ are real. Therefore, these CMs satisfy the orthogonal properties of radiation by the following three equations:

$$\begin{aligned} &< \mathbf{J}_m, R\mathbf{J}_n >= \delta_{mn} \\ &< \mathbf{J}_m, X\mathbf{J}_n >= \lambda_n\delta_{mn} \\ &< \mathbf{J}_m, Z\mathbf{J}_n >= (1+j\lambda_n)\delta_{mn} \end{aligned} \tag{2}$$

where $< B,C >= \oiint B\cdot C\,ds$ and δ_{mn} is the Kronecker delta.

From CMA, the total current $\mathbf{J}$ on a conducting body can be expressed as a linear combination of the characteristic currents

$$\mathbf{J} = \sum_\mathrm{n} \alpha_\mathrm{n}\mathbf{J}_\mathrm{n} \tag{3}$$

where α_n is the modal weighting coefficient (MWC) of the n^{th} CM, and it can be calculated as

$$\alpha_\mathrm{n} = \frac{< \mathbf{J}_\mathrm{n}, \mathbf{E}^\mathrm{i}_{\mathrm{tan}} >}{1+\mathrm{j}\lambda_\mathrm{n}} \tag{4}$$

where $\mathbf{E}^\mathrm{i}_{\mathrm{tan}}$ is the incident tangential E-field. The value of α_n determines how well the n^{th} CM is excited. The numerator of the MWC is the modal excitation coefficient (MEC). This can be defined as (5) and is determined by how similarly a coupling element excites the n^{th} CM. The denumerator of the MWC is related to the modal significance (MS) that satisfies (6), and it is determined by the resonant properties of the CM.

$$MEC = < \mathbf{J}_n, \mathbf{E}^i > \tag{5}$$

$$MS = \left| \frac{1}{1+j\lambda_n} \right| \tag{6}$$

B. Characteristic current point correlation

The characteristic current correlation is used to track the CM over frequency [21], or to find the MWC of the CM [22]. Like the characteristic current correlation, the characteristic current point correlation between the n^{th} CM and the m^{th} CM at the p^{th} triangle mesh of the PEC can be defined as

$$\rho_{mn}^{(\mathrm{p})} = \frac{< \mathbf{J}_m^{(\mathrm{p})}, \mathbf{J}_n^{(\mathrm{p})} >}{\left\| \mathbf{J}_m^{(\mathrm{p})} \right\| \left\| \mathbf{J}_n^{(\mathrm{p})} \right\|} \tag{7}$$

where the superscript (p) indicates the scalar or vector at the position of the p^{th} triangle mesh. The characteristic current point correlation can be used as interpreting the MEC similarity of two CMs. As shown in Fig. 2, if the $\mathbf{J}_n^{(\mathrm{p})}$ is not orthogonal to the $\mathbf{J}_m^{(\mathrm{p})}$, then the $\mathbf{J}_n^{(\mathrm{p})}$ can be expressed as a linear combination of the $\mathbf{J}_m^{(\mathrm{p})}$ and its orthogonal vector $\mathbf{J}_m^{(\mathrm{p})\perp}$ as

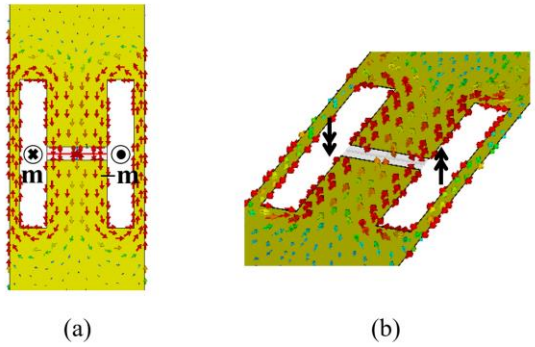

Fig. 3. Geometry of the H-shaped ICE [24]. (a) Top view, (b) 3D view.

$$\mathbf{J}_n^{(\mathrm{p})} = \frac{<\mathbf{J}_m^{(\mathrm{p})}, \mathbf{J}_n^{(\mathrm{p})}>}{\left\|\mathbf{J}_m^{(\mathrm{p})}\right\|\left\|\mathbf{J}_m^{(\mathrm{p})}\right\|}\mathbf{J}_m^{(\mathrm{p})} + t\,\mathbf{J}_m^{(\mathrm{p})\perp} = \frac{\left\|\mathbf{J}_n^{(\mathrm{p})}\right\|}{\left\|\mathbf{J}_m^{(\mathrm{p})}\right\|}\rho_{mn}^{(\mathrm{p})}\,\mathbf{J}_m^{(\mathrm{p})} + t\,\mathbf{J}_m^{(\mathrm{p})\perp} \quad (8)$$

where t is an arbitrary constant. If the $\mathbf{E}^i_{\tan}$ has the same direction as the $\mathbf{J}_m^{(\mathrm{p})}$ as shown in Fig. 2, we can derive the MEC of the n[th] CM in terms of the $\mathbf{J}_m$ as

$$<\mathbf{J}_n, \mathbf{E}^i_{\tan}> = \sum_{p=1}^{T} < \frac{\left\|\mathbf{J}_n^{(\mathrm{p})}\right\|}{\left\|\mathbf{J}_m^{(\mathrm{p})}\right\|}\rho_{mn}^{(\mathrm{p})}\mathbf{J}_m^{(\mathrm{p})} + t\,\mathbf{J}_m^{(\mathrm{p})\perp}, \mathbf{E}^{i\_(p)}_{\tan} >$$

$$= \sum_{p=1}^{T} < \frac{\left\|\mathbf{J}_n^{(\mathrm{p})}\right\|}{\left\|\mathbf{J}_m^{(\mathrm{p})}\right\|}\rho_{mn}^{(\mathrm{p})}\mathbf{J}_m^{(\mathrm{p})}, \mathbf{E}^{i\_(p)}_{\tan} > \quad (9)$$

where T is the number of the triangle mesh. If the $\mathbf{E}^i_{\tan}$ by the coupling element is dominant around this coupling element and no significant change occurs in the characteristic currents around the coupling element, we can consider (9) as follows:

$$<\mathbf{J}_n, \mathbf{E}^i_{\tan}> \approx \frac{\left\|\mathbf{J}_n^{(CE)}\right\|}{\left\|\mathbf{J}_m^{(CE)}\right\|}\rho_{mn}^{(CE)} <\mathbf{J}_m, \mathbf{E}^i_{\tan}> \quad (10)$$

where the superscript (CE) means the scalar or vector near the coupling element, which can be assumed to have a constant value near the CE. Equation (10) implies that the MECs of the m[th] and n[th] CMs have a linear relationship in terms of the characteristic current point correlation. Thus, assuming that only two m[th] and n[th] dominant CMs exist and the coupling element is designed to fully excite the m[th] CM, the total current on the conductor consists of not only the m[th] CM, but also the n[th] CM as

$$\mathbf{J} = \sum_k \frac{<\mathbf{J}_k, \mathbf{E}^i_{\tan}>}{1+j\lambda_k}\mathbf{J}_k = \frac{<\mathbf{J}_m, \mathbf{E}^i_{\tan}>}{1+j\lambda_m}\mathbf{J}_m + \frac{<\mathbf{J}_n, \mathbf{E}^i_{\tan}>}{1+j\lambda_n}\mathbf{J}_n$$

$$\approx \frac{<\mathbf{J}_m, \mathbf{E}^i_{\tan}>}{1+j\lambda_m}\mathbf{J}_m + \frac{\left\|\mathbf{J}_n^{(CE)}\right\|}{\left\|\mathbf{J}_m^{(CE)}\right\|}\rho_{mn}^{(CE)}\frac{<\mathbf{J}_m, \mathbf{E}^i_{\tan}>}{1+j\lambda_n}\mathbf{J}_n \quad (11)$$

C. Coupling element

A MIMO antenna using CMA has two design options for exciting a CM on the structure of the antenna: one employs inductive coupling elements (ICE), and the other uses capacitive coupling elements (CCE) [23]. The CCE requires an additional component, whereas the ICE does not require any additional components because it can be simply obtained by making slots on the structure. For this reason, we utilize the ICE as the foundation of the design in this paper.

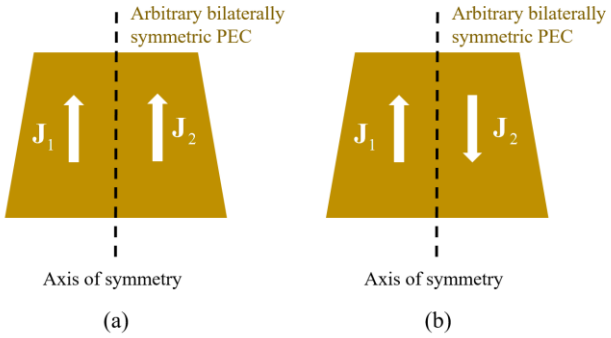

Fig. 4. Definition of even CM and odd CM for the bilaterally symmetric conductor. (a) Even CM, (b) odd CM.

As an example of the ICE, [24] qualitatively suggests that the ICE design with an H-shaped slot can excite the desired CM more. As shown in Fig. 3, when the H-shaped ICE is excited, loop currents are formed on both sides, which can be modeled as the vertical magnetic dipole sources. Since these equivalent sources exist on both sides, desired CM is created more than the ICE presented in [23]. In this paper, this H-shaped ICE is applied to the antenna to be introduced in section IV.

III. Proposed Design Method on an Electrically Small and Bilaterally Symmetric Structure

When CMA is applied to a bilaterally symmetric conductor, the CMs of the conductor can be divided into two groups with respect to the axis of symmetry, an even CM, and an odd CM [11]. As shown in Fig. 4, the total current flowing on the conductor can be divided into the currents flowing on the left side, $\mathbf{J}_1$, and currents flowing on the right side, $\mathbf{J}_2$. The even CM is defined as a CM that has a current distribution of $\mathbf{J}_1 = \mathbf{J}_2$, and odd CM is defined as a CM that has a current distribution of $\mathbf{J}_1 = -\mathbf{J}_2$. The presence of even CM and odd CM on a bilaterally symmetric conductor is proved in the appendix. In this section, a multiport MIMO antenna design method on an electrically small and bilaterally symmetric conductor based on the properties of even and odd CM is proposed.

A. Separation among antennas using the different CM groups (even and odd CMs)

Because of the symmetric nature of the even and odd CMs, separating between antennas using the different CM groups is possible by properly designing the ICEs. The term "separation" refers to a condition that satisfy both individual excitation of the CM for each antenna and low coupling between the antennas. To separate these antennas, the ICEs are designed on the axis of symmetry as shown in Fig. 5. For the antenna using the even CM, the ICE is should be on the line of the axis of symmetry as shown in Fig. 5-(a). For the antenna using the odd CM, the ICE should be perpendicular to the axis of symmetry as shown in Fig. 5-(b). Though it is unnecessary to design the slot as a rectangular shape as shown in Fig. 5, the slot should be formed symmetrically with respect to the axis of symmetry. If the above condition is satisfied, the ICE as shown in Fig. 5-(a) excites only the even CMs, and the ICE as shown in Fig. 5-(b) excites only the odd CMs because of the properties of symmetry. In

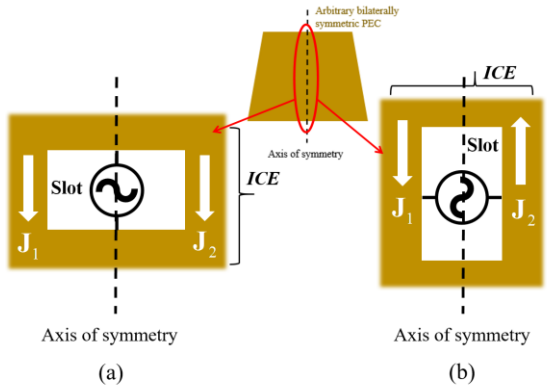

Fig. 5. Placement of the ICE. (a) ICE for exciting the even CMs, (b) ICE for exciting the odd CMs.

addition, due to their structural orthogonality, the ports between these two ICEs are virtually open, thus ensuring low coupling between ports.

B. Separation among antennas using the same CM group (even or odd CMs)

If we separate among the antennas using the different CM groups, a 2-port MIMO antenna design can be implemented easily. However, for an extension to a multiport MIMO antenna, the multiple even or odd CMs must be used individually for each antenna. Therefore, the antennas using the same CM group are necessary to be separated. However, the method used in section III-A does not guarantee separation among these antennas, and the primary reason for this is that the characteristic current point correlation of the same CM group is mostly nonzero around the ICE. Therefore, the designed ICE cannot excite the desired CM individually. Additionally, among these ICEs, a high rate of coupling exists because they excite not only the same dominant modes, but also same higher-order modes, which increases coupling.

For these reasons, the proposed solution is utilization of an MDN. By using the information of CMA, a simple MDN design can be created. The first step is to determine the position and shape of the ICE based on the information of CMA, especially the characteristic current point correlation. Knowing the characteristic current point correlation means knowing the ratio of the generated CMs by the ICE. It implies that the ICE can be designed to make the MDN easy to configure by matching the ratio. When there are only two CMs in the same CM group, the MDN design using unequal 180° hybrid coupler can be done as follows. First, the characteristic current point correlation at the entire conductor is calculated. Second, two positions for the ICEs are determined that matches the ratio of the CMs and the signal ratio of the hybrid coupler. Finally, two ICEs are designed iteratively at the obtained areas to more precisely meet the ratio that hybrid coupler is required. After design of the ICEs, the final step is to design the unequal 180° hybrid coupler for the MDN. The detailed explanation of relationship between the characteristic current point correlation and the unequal 180° hybrid coupler is as follows.

It is assumed that there are only two dominant CMs in the same CM group. To design two element MIMO antennas, two ICEs are required; ICE1 and ICE2. The currents produced or received by each ICE are called $\mathbf{J}_{\mathrm{ICE1}}$ and $\mathbf{J}_{\mathrm{ICE2}}$, and the

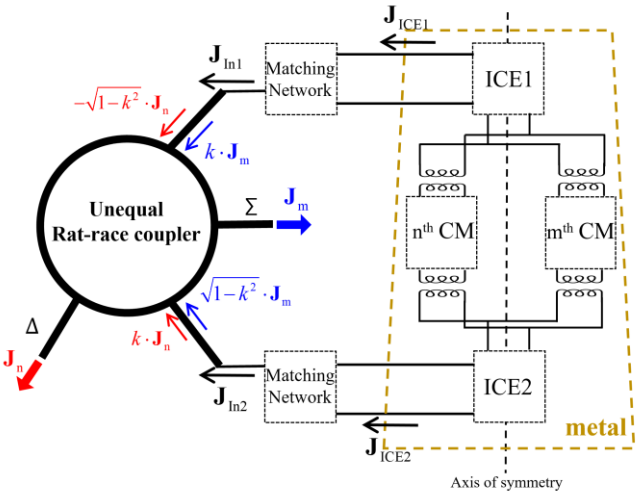

Fig. 6. Configuration of the MDN using rat-race coupler to separate the antenna using the same CM group.

incident E-fields produced by each ICE are called $\mathbf{E}^{\mathrm{i}}_{\mathrm{ICE1}}$ and $\mathbf{E}^{\mathrm{i}}_{\mathrm{ICE2}}$. Since ρ_{mn} is typically nonzero, $\mathbf{J}_{\mathrm{ICE1}}$ and $\mathbf{J}_{\mathrm{ICE2}}$ can be obtained using (11) as

$$\mathbf{J}_{\mathrm{ICE1}} \approx \frac{<\mathbf{J}_m, \mathbf{E}^{\mathrm{i}}_{\mathrm{ICE1}}>}{1+j\lambda_m}\mathbf{J}_m + \frac{<\mathbf{J}_n, \mathbf{E}^{\mathrm{i}}_{\mathrm{ICE1}}>}{1+j\lambda_n}\mathbf{J}_n$$

$$\approx \frac{<\mathbf{J}_m, \mathbf{E}^{\mathrm{i}}_{\mathrm{ICE1}}>}{1+j\lambda_m}\mathbf{J}_m + \frac{\left\|\mathbf{J}_n^{(\mathrm{ICE1})}\right\|}{\left\|\mathbf{J}_m^{(\mathrm{ICE1})}\right\|}\rho_{mn}^{(\mathrm{ICE1})}\frac{<\mathbf{J}_m, \mathbf{E}^{\mathrm{i}}_{\mathrm{ICE1}}>}{1+j\lambda_n}\mathbf{J}_n \quad (12)$$

$$\mathbf{J}_{\mathrm{ICE2}} \approx \frac{<\mathbf{J}_m, \mathbf{E}^{\mathrm{i}}_{\mathrm{ICE2}}>}{1+j\lambda_m}\mathbf{J}_m + \frac{<\mathbf{J}_n, \mathbf{E}^{\mathrm{i}}_{\mathrm{ICE2}}>}{1+j\lambda_n}\mathbf{J}_n$$

$$\approx \frac{\left\|\mathbf{J}_m^{(\mathrm{ICE2})}\right\|}{\left\|\mathbf{J}_n^{(\mathrm{ICE2})}\right\|}\rho_{mn}^{(\mathrm{ICE2})}\frac{<\mathbf{J}_n, \mathbf{E}^{\mathrm{i}}_{\mathrm{ICE2}}>}{1+j\lambda_m}\mathbf{J}_m + \frac{<\mathbf{J}_n, \mathbf{E}^{\mathrm{i}}_{\mathrm{ICE2}}>}{1+j\lambda_n}\mathbf{J}_n \quad (13)$$

where the superscript (ICE) refers to the vector or scalar near the ICE. As mentioned, the MDN is designed using the conventional unequal (or equal) 180° hybrid coupler, especially rat-race coupler (RRC). The RRC outputs the signals for $\mathbf{J}_{\mathrm{m}}$ on the Σ-port and $\mathbf{J}_{\mathrm{n}}$ on the Δ-port from the two input signals $\mathbf{J}_{\mathrm{In1}}$, and $\mathbf{J}_{\mathrm{In2}}$ respectively as

$$\mathbf{J}_{\mathrm{In1}} = ck\mathbf{J}_m - c\sqrt{1-k^2}\mathbf{J}_n \quad (14)$$

$$\mathbf{J}_{\mathrm{In2}} = c\sqrt{1-k^2}\,\mathbf{J}_m + ck\mathbf{J}_n \quad (15)$$

where c is an arbitrary constant and k is the coupling coefficient of the RRC [25]. As shown in Fig. 6, if two ICEs exciting two combined CMs are connected to the RRC, the signal coming from each ICE to the inputs of the RRC are as (12) and (13). When these incoming signals of the RRC satisfy (14) and (15), the individual CMs are generated at the output terminals of the RRC. That is, if the ICE is designed to satisfy the conditions $\mathbf{J}_{\mathrm{ICE1}} = \mathbf{J}_{\mathrm{In1}}$, and $\mathbf{J}_{\mathrm{ICE2}} = \mathbf{J}_{\mathrm{In2}}$ (or $\mathbf{J}_{\mathrm{ICE1}} = \mathbf{J}_{\mathrm{In2}}$, and $\mathbf{J}_{\mathrm{ICE2}} = \mathbf{J}_{\mathrm{In1}}$), the two combined CMs from the ICE can be separated through the RRC. The results for the above equations are as follows.

$$\frac{\left\|\mathbf{J}_n^{(\mathrm{ICE1})}\right\|}{\left\|\mathbf{J}_m^{(\mathrm{ICE1})}\right\|}\rho_{mn}^{(\mathrm{ICE1})}\left|\frac{1}{1+j\lambda_n}\right|^2 = -\frac{\left\|\mathbf{J}_m^{(\mathrm{ICE2})}\right\|}{\left\|\mathbf{J}_n^{(\mathrm{ICE2})}\right\|}\rho_{mn}^{(\mathrm{ICE2})}\left|\frac{1}{1+j\lambda_m}\right|^2 \quad (16)$$

$$\frac{< \mathbf{J}_m, \mathbf{E}^{\mathrm{i}}_{\mathrm{ICE1}} >}{1+ j\lambda_m} = \frac{< \mathbf{J}_n, \mathbf{E}^{\mathrm{i}}_{\mathrm{ICE2}} >}{1+ j\lambda_n} \quad (17)$$

$$k = \frac{\left| \frac{1}{1+ j\lambda_m} \right|}{\sqrt{\left(\frac{1}{1+ j\lambda_m} \right)^2 + \left(\frac{\left\| \mathbf{J}_n^{(\mathrm{ICE1})} \right\|}{\left\| \mathbf{J}_m^{(\mathrm{ICE1})} \right\|} \frac{\rho_{mn}^{(\mathrm{ICE1})}}{1+ j\lambda_n} \right)^2}} \quad . \quad (18)$$

Equation (16) depends only on the parameters of CMA. λ_m and λ_n are determined by the operating frequency. So, when the desired frequency is determined, the positions of ICE1 and ICE2 that satisfy (16) are found on the axis of symmetry. (17) is related to MECs by each ICE, and it depends on the position and shape of the ICE. Since the position of the ICEs is derived from the (16), the shape of the ICE is determined to satisfy (17) through the iterative EM simulation process. Finally, the coupling coefficient of the RRC is determined by (18). (18) consists of the parameters of the CMA determined after the position of the ICE is selected by (16).

In conclusion, by designing an ICE and RRC that satisfy the above three equations, individual CMs can be extracted at the output of the RRC. According to the reciprocity theorem, if the signal is applied to the Σ-port as a transmitting mode, it radiates through an antenna corresponding to m$^{\mathrm{th}}$ CM. Similarly, if the signal is applied to the Δ-port, it radiates through an antenna corresponding to n$^{\mathrm{th}}$ CM. In addition, the RRC guarantees isolation between two inputs or two outputs when all ports are connected to a 50 Ω system [25], which ensures high isolation between antennas using the same CM group.

C. The proposed multiport MIMO antenna system configuration

Fig. 7 shows the system configuration for the proposed multiport MIMO antenna on an electrically small and bilaterally symmetric conductor. Fig. 7-(a) is a system configuration of a 2-port MIMO antenna. Here, one antenna uses an even CM, and the other antenna uses an odd CM. As mentioned in the section III-A, the IC E design is sufficient for separating antennas using the different CM groups. Fig. 7-(b) shows the system configuration of a 3-port MIMO antenna. Here, the two antennas use different even CMs individually, and the other antenna uses an odd CM. Similarly, the antenna using odd CMs is designed with the ICE alone. However, for the antennas using the different even CMs, an additional MDN is required, as described in section III-B. When the two antennas use different odd CMs individually and the other antenna uses an even CM, the system configuration is same as shown in Fig. 7-(b), except designing a MDN at the odd CM part rather than the even CM part. While the existing method requires a 6-port MDN with 3 inputs and 3 outputs [15], the proposed systematic design requires only a 4-port MDN with 2 inputs and 2 outputs, which can reduce the design complexity of the MDN. Fig. 7-(c) is a system configuration of a 4-port MIMO antenna and it can be only applied when two even CMs and two odd CMs are used as individual antennas. Even in this case, however, a much simpler implementation is possible because two 4-port MDNs are required compared to the existing methods requiring an 8-port MDN [16].

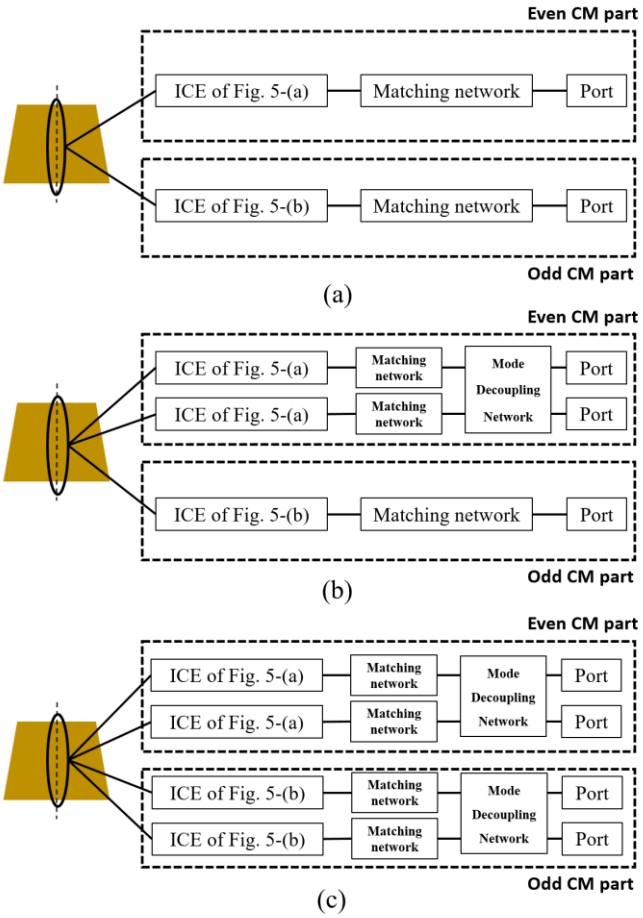

Fig. 7. Systematic configuration of the proposed MIMO antenna. (a) 2-port MIMO antenna system using one even CM and one odd CM, (b) 3-port MIMO antenna system using two even CMs and one odd CM, (c) 4-port MIMO antenna system using two even CMs and two odd CMs.

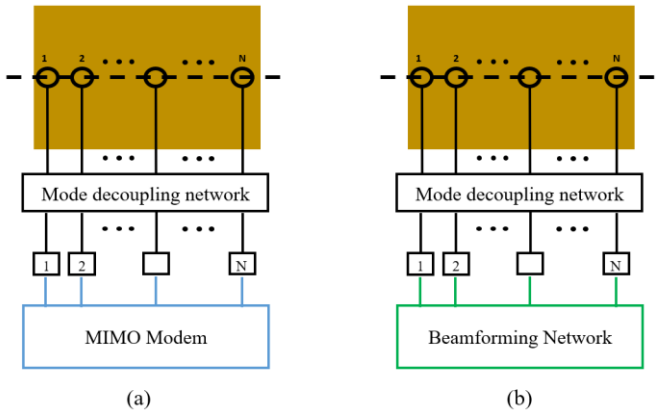

Fig. 8. Dual function of the proposed MIMO antenna. (a) MIMO Communication system, (b) Beamforming system

IV. CAPABILITIES OF BEAMFORMING USING THE PROPOSED MULTI-PORT ANTENNA

The proposed multiport antenna can be not only used to the MIMO communication on using MIMO modem, but also perform a function of beamforming antenna using a beamforming network shown in Fig. 8. For the desired direction of beamforming, the weighting factor must be chosen properly.

In this paper, the weighting factor is determined based on the least square method as below.

Consider a N-port chassis antenna with N characteristic modes as shown in Fig. 1. Assuming that each port excites one pure characteristic mode respectively, all ports are decoupled and have the same phase center, the N-port pattern matrix **A** can be denoted as

$$\mathbf{A}=\left[\mathbf{f}_1^{CM} \quad ... \quad \mathbf{f}_N^{CM}\right] \tag{19}$$

where $\mathbf{f}_i^{CM}(\psi)\in\mathbf{C}^M$ is the vector representation of radiation pattern of the i-th characteristic mode $f_i^{CM}(\theta,\phi)$. Then, the radiation pattern of the N-port chassis antenna is

$$\mathbf{F}=\mathbf{A}\mathbf{w} \tag{20}$$

where $\mathbf{w}=[w_1\ w_2\ \ldots\ w_N]^T\in\mathbf{C}^N$ is the complex weighting vector of the N-port system. Thus, the desired radiation pattern of the N-port chassis antenna $\mathbf{F}_D$ is determined by finding the proper vector **w** given **A** satisfying $\mathbf{F}_D=\mathbf{A}\mathbf{w}$. This overdetermined system of linear equations can be approximated by solving the least square problem as:

$$\min_{\mathbf{w}}\left\|\mathbf{F}_D-\mathbf{A}\mathbf{w}\right\|_2 \tag{21}$$

The least squares solution of (21) **w*** is

$$\mathbf{w}^*=\left[\mathbf{A}^H\mathbf{A}\right]^{-1}\mathbf{A}^H\mathbf{F}_D \tag{22}$$

Since the patterns of characteristic modes are all orthogonal as $(\mathbf{f}_i^{CM})^H\ \mathbf{f}_j^{CM}=\delta_{ij}$ resulting in $\mathbf{A}^H\mathbf{A}=\mathbf{I}$, the solution can be simplified as

$$\mathbf{w}^*=\mathbf{A}^H\mathbf{F}_D \tag{23}$$

Therefore, given the N-port pattern matrix **A**, the weighting vector **w** can be chosen as **w*** that depends on the desired pattern $\mathbf{F}_D$.

Without considering reality, the ideal desired pattern is to focus the field only in one direction as

$$\mathbf{F}_D=\delta(\psi_0). \tag{24}$$

Then, the chosen weighting vector is

$$\mathbf{w}^*=\mathbf{A}^H\delta=\left[f_{1,\psi_0}^{CM} \quad ... \quad f_{N,\psi_0}^{CM}\right]^H \tag{25}$$

The physical meaning of the result can be found using the reciprocity theorem. Considering a plane-wave incoming from the angle ψ_0, the received signals for N ports correspond to the scaled values of radiation patterns as

$$\mathbf{r}=c\left[f_{1,\psi_0}^{CM} \quad ... \quad f_{N,\psi_0}^{CM}\right]^T \tag{26}$$

where c is an arbitrary constant. Comparing (25) with (26), the chosen weighting vector is same as the phase conjugation of the received signal **r**. In other words, the weighting vector is chosen as the time-reversal of the narrow-band received signal.

V. Conclusion

In this paper, a simple multiport MIMO antenna design method on an electrically small and bilaterally symmetric conductor is proposed. The simple design is provided by separating antennas using CMs of the different groups with the properly designed ICEs. For this reason, only the separation of the antennas using the different CMs of the same group is needed, and it is sufficient to use a conventional unequal RRC design for some cases. To use MDN as the RRC, the conditions for the ICE designs are suggested mathematically. In the case of a 3-port MIMO antenna using two even CMs and one odd CM (or two odd CMs or one even CM), it is possible to easily implement an MDN through only one RRC. In the case of a 4-port MIMO antenna using two even CMs and two odd CMs, it is possible to easily implement an MDN using two RRCs. In fact, for any N-port MIMO antenna, the separation of between antennas using even and odd CMs using the ICE design proposed in section III-A enables the design of a simpler MDN than the existing design methods, but this could still be complex. So, the design of the N-port MIMO antenna on an electrically large structure should be studied in the future. In addition to the functionality of MIMO communication, the proposed antenna can perform a function of beamforming based on the least square method. As a result, the proposed design method can be applied to many electrically small and bilaterally symmetric platforms, such as cars, airplanes, and ships.

References

[1] L. Zheng, and N. C. Tse, "Diversity and multiplexing: A fundamental tradeoff in multiple-antenna channels," *IEEE Trans. Inf. Theory*, vol. 49, no. 5, pp. 1073–1096, May 2003.

[2] R. Garbacz and R. Turpin, "A generalized expansion for radiated and scattered fields," *IEEE Trans. on Antennas and Propag.*, vol. 19, no. 3, pp. 348-358, May 1971.

[3] R. F. Harrington, and J. R. Mautz, "Theory of characteristic modes for conducting bodies," *IEEE Trans. Antennas Propag.*, vol. 19, no. 5, pp. 622–628, Sept. 1971.

[4] Y. Chen, and C. Wang, "Electrically small UAV antenna design using characteristic modes," *IEEE Trans. Antennas Propag.*, vol. 62, no. 2, pp. 535–545, Feb. 2014.

[5] Y. Chen, and C. Wang, "HF band shipboard antenna design using characteristic modes," *IEEE Trans. Antennas Propag.*, vol. 63, no. 3, pp. 1004–1013, March 2015.

[6] T Shih, and N. Behdad, "Bandwidth enhancement of platform-mounted HF antennas using characteristic mode theory," *IEEE Trans. Antennas Propag.*, vol. 64, no. 7, pp. 2648–2659, July 2016.

[7] K. K. Kishor, and S. V. Hum, "A pattern reconfigurable chassis-mode MIMO antenna," *IEEE Trans. Antennas Propag.*, vol. 62, no. 6, pp. 3290–3298, Jun. 2014.

[8] H. Li, Z. Miers, and B. K. Lau, "Design of orthogonal MIMO handset antennas based on characteristic mode manipulation at frequency bands below 1 GHz," *IEEE Trans. Antennas Propag.*, vol. 62, no. 5, pp 2756–2766, May 2014.

[9] I. Szini, A. Tatomirescu, and G. F. Pedersen, "On small terminal MIMO antennas, harmonizing characteristic modes with ground plane geometry," *IEEE Trans. Antennas and Propag.*, vol. 63, no. 4, pp. 1487–1497, April 2015.

[10] C. Deng, Z. Feng, and S. V. Hum, "MIMO mobile handset antenna merging characteristic modes for increased bandwidth," *IEEE Trans. Antennas Propag.*, vol. 64, no. 7, pp. 2660–2667, July 2016.

[11] B. Yang, and J. J. Adamas, "Systematic shape optimization of symmetric MIMO antennas using characteristic modes," *IEEE Trans. Antennas Propag.*, vol. 64, no. 7, pp. 2668–2678, July 2016.

[12] M. Bouezzeddine, and W. L. Schroeder, "Design of a wideband, tunable 4-port MIMO antenna system with high isolation based on the theory of characteristic modes," *IEEE Trans. Antennas Propag.*, vol. 64, no. 7, pp. 2679–2688, July 2016.

[13] R. Martens, and D. Manteuffel, "Systematic design method of a mobile multiple antenna system using the theory of characteristic modes," *IET Microwaves, Antennas & Propag.*, vol. 8, no. 12, pp. 887–893, Sept. 16 2014.

[14] D. Manteuffel, and R. Martens, "Compact multimode multielement antenna for indoor UWB massive MIMO," *IEEE Trans. Antennas Propag.*, vol. 64, no. 7, pp. 2689–2697, July 2016.

[15] C. Volmer, J. Weber, R. Stephan, K. Blau, and M. A. Hein, "An eigen-analysis of compact antenna arrays and its application to port decoupling," *IEEE Trans. Antennas and Propag.*, vol. 56, no. 2, pp. 360–370, Feb. 2008.

[16] J. C. Coetzee, and Y. Yu, “Port decoupling for small arrays by means of an eigenmode feed network,” *IEEE Trans. on Antennas and Propag.*, vol. 56, no. 6, pp. 1587-1593, June 2008.
[17] A. Krewski, and W. L. Schroeder, “N-port DL-MIMO antenna system realization using systematically designed mode matching and mode decomposition network,” *2012 42nd European Microwave Conference*, Amsterdam, the Netherlands, Oct. 29–Nov. 1, 2012, pp. 156-159.
[18] J. Ethier, and D. A. McNamara, “An interpretation of mode-decoupled MIMO antennas in terms of characteristic port modes,” *IEEE Trans. Magn.*, vol. 45, no. 3, pp. 1128–1131, Mar. 2009.
[19] D. W. Kim, and S. Nam, "Design of Chassis MIMO Antenna Using Characteristic Mode Theory," *2017 International Symposium on Antennas and Propagation (ISAP)*, Phuket, Thailand, Oct. 30–Nov. 2, 2017.
[20] D. W. Kim, and S. Nam, “Systematic design of 3-port bug-like MIMO antenna based on theory of characteristic mode,” *2017 11th European Conference on Antennas and Propagation (EUCAP)*, Paris, France, Mar. 19–24, 2017, pp. 2224-2227.